International Journal of Industrial Electronics, Control and Optimization © 2020 IECO
Vol. 3, No. 3, pp. 223-234, July (2020)

# Coordination of adaptive distance protection in transmission and wind farm collector lines under resistive fault conditions

Jamshid Barati[1], Seyed Ghodratollah Seifossadat[2,†], and Mahmood Joorabian [3]

[1,2,3] Department of Electrical Engineering, Faculty of Engineering, Shahid Chamran University of Ahvaz, Iran

**ABSTRACT**

*Distance relays calculate the path impedance between the fault point and the relay location by sampling the voltage and current at the relay location. By using the ratio of the impedance estimated by the relay to the impedance of the line where the relay is installed, the location of the fault can be estimated by a distance relay. However, several factors influence the estimated impedance and proper operation of distance relays. The most important of these factors is the resistive fault occurrence, which results in an increase in the impedance and deviation of the impedance estimated by the relay as well as causes relay under-reach. Therefore, in the present study, an adaptive method is proposed to modify the protection zones of distance relays settings under different operating conditions and resistive single-line-to-ground (SLG) fault occurrence. Furthermore, the adaptive distance protection of transmission lines, wind farm collector lines and the protection coordination of the relays in these lines are investigated. In this method, an adaptive coefficient is added to the conventional characteristics of distance relays to improve the accuracy and coordination. The proposed adaptive method can also maintain the coordination of different protection zones of primary and backup relay pairs. In addition to analytical verification, the numerical results obtained from simulation show the efficiency of the proposed method. The proposed method is implemented on a power system with transmission lines and wind farms and simulated in MATLAB/Simulink environment.*

**Article Info**

***Keywords:*** Adaptive Characteristic, Coordination, Distance Relay, Fault Resistance, Wind Farm

***Article History:***
**Received** 2019-08-26
**Accepted** 2019-12-20

## I. INTRODUCTION

Distance relays are the most important protection equipment in transmission lines. The stability of power systems is also highly dependent on the proper operation of these relays. Distance relays calculate the equivalent impedance of the network using the ratio of voltage to current phasors measured at their location. By comparing this impedance with the impedance of the line in which the relay is installed, fault occurrence can be detected. Indeed, in the event of a zero-resistance fault along this line, the impedance of the path from the fault location to the relay location becomes smaller than the impedance of the line and fault occurrence is detected. The operating characteristics of distance relays are affected by the changes in the network structure and operating conditions [1]. For example, power fluctuations, multiterminal lines, reactive power compensation in lines, fault impedance, etc., are some uncertainties affecting the operation of distance relays [2].

In many recent studies, operating characteristics of distance relays have been modified so that their operation become robust against the mentioned uncertainties. In [3], the fault impedance of line seen by a distance relay is determined using ANN method. In parallel transmission lines, since the line impedance is affected by mutual coupling of parallel circuits, a reduction in sensitivity or miscoordination is possible. In [4], a high-accuracy protective approach is presented for parallel transmission lines.

In [5], [6], a protection scheme is proposed to overcome the

†CorrespondingAuthor: seifossadat@yahoo.com
Tel: +98-9166182789, Department of Electrical Engineering, Faculty of Engineering, Shahid Chamran University of Ahvaz, Ahvaz, Iran

effect of fault resistance on the impedance seen by a relay. In [7], [8] a method is proposed to reduce the effects of fault resistance on the impedance seen by the relays in long transmission lines. In [9], a hybrid method is implemented to detect faults with impedance using resistance amplitude and voltage-current characteristics. In [10], a novel digital distance relay is proposed to increase the accuracy of the conventional distance protection in the case of a high impedance fault occurrence.

The Doubly-Fed Induction Generators (DFIG) based Wind Turbines (WT) are widely used in WTs connected to power systems [11]. In addition, wind farms based on doubly fed induction generators (DFIGs) are widely employed in existing power networks [12]. In wind farms, wind generators are connected to the low-voltage side of step-up transformers in parallel in sets of 5 to 10 generators. They are then connected to step-up substations of wind farms by means of 10kV or 35 kV collector lines. The protection of transmission and collector lines is of great importance. In the event of untimely operation of primary protection (low sensitivity) or improper operation of backup protection (miscoordination), extensive blackouts may happen in the network. However, because the collector lines are grounded by means of a resistance or arc suppression coil, in the event of a fault, the fault resistance strongly affects the operation of distance relays [10]. In conventional protection schemes for collector lines, overcurrent relays are usually used on one side of the lines and close to the transformer bus of the lines; however, the major problem with this type of protection is the possibility of miscoordination [13]. In [14], the protection of lines connecting wind farms is studied using the concept of distance protection. In this reference, the proposed new protection scheme concerns fault occurrence in multiterminal DC lines. Moreover, collector line DC voltage variations are used to distinguish AC faults from DC faults, and overcurrent protection is used to determine the type of fault.

In [15], [16], a wind farm protection scheme is proposed that provides short-circuit current protection of low-voltage collector lines and both sides (low-voltage and medium-voltage) of the transformer connecting wind farms to the network. In [17], a protection scheme is presented based on voltage - current for wind farm collector lines are proposed.

In addition, DFIG-based wind farms are widely employed in existing power networks, and Numerous studies have been performed on the distance protection performance of wind farms [18-21]. In [16-18], in addition to investigating the effect of the current injected by wind farms electronic converters in the event of a fault, the severity of the effect and the probability of malfunction of distance relays are investigated. Considering the specific fault characteristics and complex control strategies of DFIGs in wind farms, a distance relay in time domain is proposed in [19] based on the resistance-inductance (R-L) differential-equation algorithm. In [20], [21], adaptive coefficients are proposed for improving the operation of distance relays under fault conditions and in the presence of DFIGs. The performance of these methods is based on sequence components that are inefficient when resistive faults occur.

However, none of these studies have discussed the issue of coordination between the operation of transmission line relays and wind farm collector lines. Therefore, this paper proposes an adaptive protection scheme for lines connecting wind farms with doubly fed induction generators (DFIGs) in such a way that full coordination is maintained among distance protection zones 1, 2 and 3 of these lines and transmission lines. This coordination is maintained even in the event of resistive single-line-to-ground (SLG) faults and power fluctuations. In the proposed method, a set of adaptive coefficients are defined in terms of the voltage drops at the relay location and the fault occurrence point. Next, an adaptive protection scheme is presented based on a criterion that considers the relationship between the phase current measured at the relay location and the fault current. Because the voltage drop equation does not depend on fault resistance, the fault resistance will not affect the performance of the proposed method. This method is applicable to the conventional distance relays and only requires the voltage and current at the relay location. As a result, the implementation of this method requires no additional cost.

## II. PROPOSED SCHEME FOR COLLECTOR LINES PROTECTION

Doubly fed induction generators are paralleled in multiple sets and are connected to $35^{kV}/110^{kV}$ step-up transformers of transmission lines through collector lines. Transmission lines are connected to the power grid via 330 kV step-up substations.

In the event of a SLG fault in collector lines, the distance protection operates based on the diagram shown in Fig. 1.

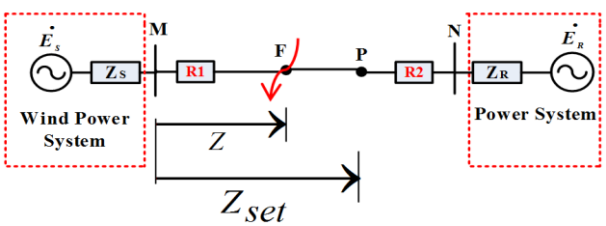



**Fig. 1**. Adaptive distance protection system.

In Fig. 1, M is in the collector system side and $\dot{E}_S$ is the equivalent system voltage; N is on the grid side and $\dot{E}_R$ is the equivalent system voltage. The equivalent system impedances in the collector and grid sides are $Z_S$ and $Z_R$, respectively.

When a SLG fault occurs on the line, the measured voltage $\dot{U}_m$ at the relay location satisfies the following equation:

$$\dot{U}_m = Z\dot{I}_m + \dot{U}_f \quad (1)$$

Where $\dot{I}_m$ is the measured current and $\dot{U}_f$ is the voltage at the fault point. By dividing both sides of (1) by $\dot{I}_m$, we have

$$Z_m = Z + \frac{\dot{U}_f}{\dot{I}_m} = Z + \frac{\dot{I}_f R_g}{\dot{I}_m} \quad (2)$$

Where $Z_m$ is the impedance measured at relay location, $\dot{I}_f$ is the fault current, and $R_g$ is the fault resistance. According to Eq. (2), the impedance $Z_m$ seen by the relay consists of two parts. The first part corresponds to the actual impedance of the fault path (Z), and the second part corresponds to the impedance caused by the fault resistance ($\frac{\dot{I}_f R_g}{\dot{I}_m}$). If the second part has a share in the impedance seen by the relay, an error occurs in the operation of the conventional distance relay and results in the reduction of sensitivity of this relay. The phasor diagram of voltage and current are shown in Fig. 2 in the event of a SLG fault in the collector lines. The parameters $\dot{U}_{M|0|}$ and $\dot{U}_{N|0|}$ are the voltages of buses M and N; $\dot{U}_{f|0|}$ is the voltage at fault occurrence point F, in the pre-fault condition; $\dot{I}_m$, $\dot{I}_n$ and $\dot{I}_f$ are the currents flowing through the collector lines, transmission lines and fault point, respectively.

$$\dot{I}_f = \dot{I}_m + \dot{I}_n \quad (3)$$

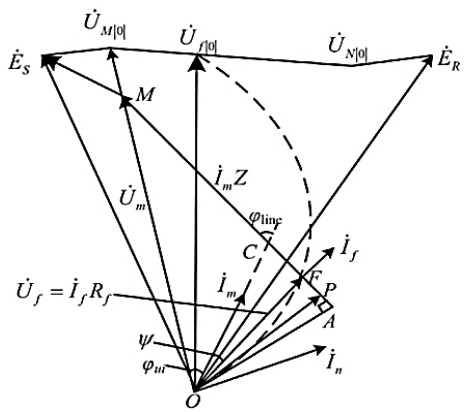



**Fig. 2**: Phasor diagram when a SLG fault occurs on collector lines.

$\psi$ is the angle difference between the measured current ($\dot{I}_m$) and the fault point voltage $\dot{U}_f$. If a fault occurs at the same location with a different fault resistance, vector $\overrightarrow{OF}$ will move along the arc with $\dot{U}_{f|0|}$ as the string. Moreover, $\overrightarrow{MF}$ still shows voltage drop on Z and has nothing to do with fault resistance. Therefore, the protection criterion formed by $\overrightarrow{MF}$ is also immune to the fault resistance. Note that C indicates the intersection point of the measured current $\dot{I}_m$ and the extension of line $\overrightarrow{MF}$. Inequalities in Eqs. (4) and (5) are based on the diagram in Fig. 2:

$$\begin{aligned} |\overrightarrow{OA}| &= |\dot{U}_m| \cos\varphi \\ |\overrightarrow{MA}| &= |\dot{U}_m| \sin(\varphi_{ui} + 90 - \varphi_{line}) \\ |\overrightarrow{FA}| &= |\dot{U}_m| \cos(\varphi_{ui} + 90 - \varphi_{line}) \tan(90 - \varphi_{line} - \psi) \end{aligned} \quad (4)$$

$$\begin{aligned} |\overrightarrow{MF}| &= |\overrightarrow{MA}| - |\overrightarrow{FA}| \\ &= |\dot{U}_m| \sin(\varphi_{ui}+90-\varphi_{line}) - |\dot{U}_m| \cos(\varphi_{ui}+90-\varphi_{line}) \tan(90-\varphi_{line}-\psi) \end{aligned} \quad (5)$$

By applying Eq. (5) to Eq. (4), the voltage drop equation can be obtained using Eq. (6):

$$\begin{aligned} |\overrightarrow{MF}| = |\dot{I}_m \times Z| &= |\dot{U}_m| \sin(\varphi_{ui} + 90 - \varphi_{line}) \\ &\quad - |\dot{U}_m| \cos(\varphi_{ui} + 90 - \varphi_{line}) \tan(90 - \varphi_{line} - \psi) \\ &= |\dot{U}_m| \frac{\sin(\varphi_{ui} + \psi)}{\cos(90 - \varphi_{line} - \psi)} \end{aligned} \quad (6)$$

By dividing both sides of Eq. (6) by the measured current amplitude ($\dot{I}_m$), Eq. (7) is obtained.

$$|Z| = |Z_m| \frac{\sin(\varphi_{ui} + \psi)}{\cos(90 - \varphi_{line} - \psi)} \quad (7)$$

Finally, the proposed adaptive coefficient $K_a$ is defined in Eq. (8) for improving the operation of distance relays of the collector lines.

$$K_a = \frac{\cos(90 - \varphi_{line} - \psi)}{\sin(\varphi_{ui} + \psi)} \quad (8)$$

where $\varphi_{line}$ is the impedance angle of collector line, and $\varphi_{ui}$ is the phase angle difference between the voltage and current measured by the relay. For a SLG fault, the fault current is equal to $\dot{I}_f$, $\dot{I}_f = 3\dot{I}_{f2} = 3\dot{I}_{f0}$. Therefore, the deviation angle $\psi$ is obtained by Eq. (9) as follows:

$$\psi = \arg\left(\frac{\dot{I}_m}{\dot{I}_f}\right) = \arg\left(\frac{\dot{I}_m}{\dot{I}_{f0}}\right) = \arg\left(\frac{\dot{I}_m}{\dot{I}_{f2}}\right) \quad (9)$$

where $\dot{I}_{f2}$ and $\dot{I}_{f0}$ are, respectively, the negative sequence and zero sequence currents at the fault point. The zero sequence equivalent circuit of the system is shown in Fig. 3, when a SLG fault occurs in the collector lines. In this figure, α is the fault occurrence location F in the collector line in percent.

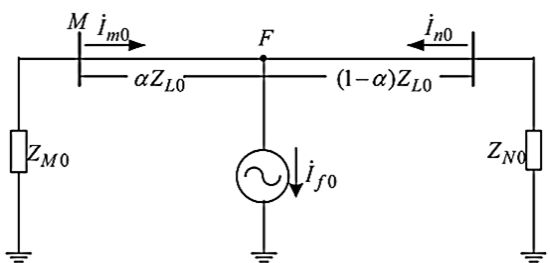



**Fig. 3**. Zero sequence equivalent network in case of SLG fault in the collector lines.

In addition, $Z_{L0}$ is the zero-sequence impedance of the lines; $Z_{N0}$ and $Z_{M0}$ are the equivalent impedances of the zero-sequence of the connection system (on the collector lines side) and the equivalent network, respectively. According to the equivalent circuit of Fig. 3, the relationship between the

zero-sequence current at the fault point ($\dot{I}_{f0}$) and the zero-sequence current at the installation point of the relay along the collector lines ($\dot{I}_{m0}$) is obtained from Eq. (9).

$$\dot{I}_{m0}=C_{m0}\dot{I}_{f0}=\frac{Z_{N0}+(1-\alpha)Z_{L0}}{Z_{M0}+Z_{N0}+Z_{L0}}\dot{I}_{f0} \quad (10)$$

where $C_{m0}$ is the zero-sequence current distribution coefficient. Because of the small share of collector lines in supplying the fault current and the independence of zero sequence impedance angle of the system from loads, the zero-sequence current distribution coefficient in Eq. (10) can be considered as a real number. Moreover, the zero-sequence current angle at the relay location can be approximated as equal to the zero-sequence current angle at the fault point. Consequently, the deviation angle defined in Eq. (9) is given as Eq. (11).

$$\psi=\arg\left(\frac{\dot{I}_m}{\dot{I}_{m0}}\right) \quad (11)$$

According to Eq. (10), the deviation angle $\psi$ depends only on the zero sequence current and the measured current at the relay location. After calculating $\psi$, the proposed adaptive coefficient can be determined using Eq. (8), and the distance relay setting can be calculated using Eq. (12).

$$\begin{cases} |Z_m|\leq K_a|Z_{set}| & \text{In - zone fault} \\ |Z_m|>K_a|Z_{set}| & \text{Out -of-zone fault} \end{cases} \quad (12)$$

where $Z_m$ is the measured impedance. $Z_{set}$ is the boundary of the protection setting range. $k_a$ is the adaptive setting coefficient. Fig. 4 shows the overall schematic diagram of the proposed adaptive distance relay. According to the flowchart of the proposed algorithm, in the first step, the voltage and current are sampled at the relay location. Then, the sampled phasors and sequence components of voltage and current signals are extracted. Next, adaptive coefficient $K_a$ is calculated based on Eq. (8), and $Z_{set}$ settings of distance relay protection zones 1, 2 and 3 are updated. Moreover, the impedance seen by the relay ($Z_m$) and the ratio of voltage and current phasors are also calculated. Next, the fault occurrence is investigated based on the updated characteristics of the relay ($Z'_{set}=K_aZ_{set}$). If a fault is detected within any of the protection zones, a trip command is sent to the corresponding power circuit breaker at a predetermined time. Finally, the relay resets and restarts to sample the voltage and current.

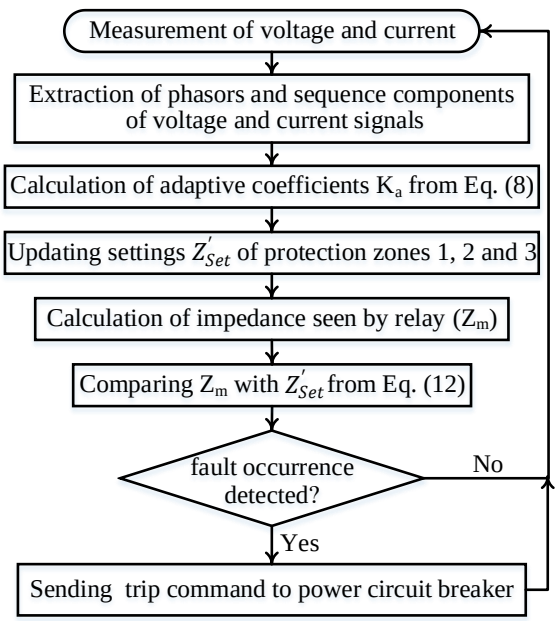



**Fig. 4**. Proposed adaptive distance relay algorithm.

## III. Simulation Results

In this section, the operation of the proposed method is simulated for a variety of power system configurations including radial (Single–source), double-source and the network connected to the wind farm. Next, the results of these evaluations are analyzed separately for each configuration.

### *A. Network with Radial Configuration*

The specifications of the radial network under study shown in Fig. 20 is given in the appendix. In this network, a distance relay is installed at the beginning of the transmission line close to bus M. To determine the setting of this relay, a fault without resistance is modeled somewhere at the end of the line (close

to bus N). The fault impedance seen by the relay is measured and stored as its setting. In Fig. 5, the effect of fault resistance on the fault impedance seen by the relay is investigated.

A fault is modeled at 0.25 seconds, so the system is in a steady-state; however, due to the use of Fourier transform for calculating sequence components of phases, there exists a one-cycle time delay after the fault in waveforms. In Fig. 5, the location of the fault is fixed at 0.25 of transmission line length. Then, the occurrence of faults with resistances of 0, 50 and 300 ohms is studied. As can be seen, in all cases, the value of the relay setting has increased in proportion to the impedance seen by the relay. Accordingly, the fault impedances seen by the relay for faults with resistances of 0, 50 and 300 ohms are 26.16, 70.68 and 362.2 ohms, respectively. As a result, the adaptive impedance settings of the relay increase to 109, 289.9 and 1386 ohms, respectively. In all these cases, almost the same ratio of 0.25 is maintained between the fault impedance seen by the relay and the relay impedance setting.

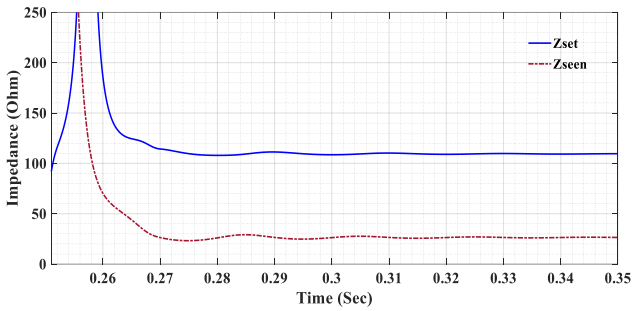



**Fig. 5(a)** occurrence of fault with no resistance

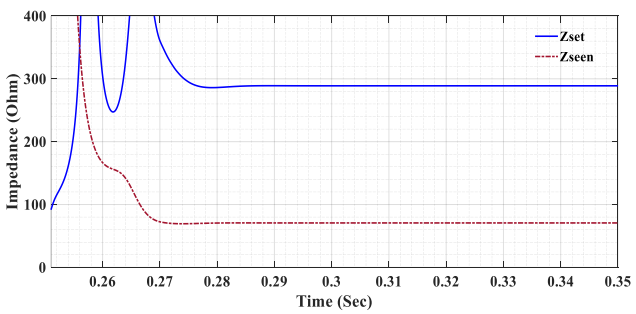



**Fig. 5(b)** fault with a resistance of 50 ohm

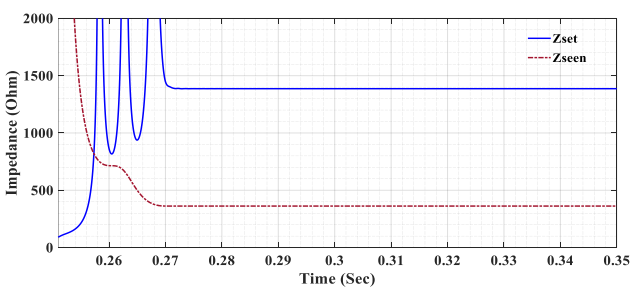



**Fig. 5(c)** fault with a resistance of 300 ohm

**Fig. 5.** Fault occurrence at 0.25 of transmission line length with different resistances in radial network.

In addition, these calculations are repeated for the faults occurring at 0.75 of the transmission line length with resistances of 0, 10, 50 and 300 ohms. According to the results in Fig. 6, it can be seen that, in all cases, the adaptive settings of the relay have increased proportional to the increase in fault resistance, and the fault occurrence location (0.75 of the transmission line length) has been detected accurately. If the fault resistance increases from zero to 50 and 300 ohms, the impedance seen by the relay increases from 79.33 to 108.5 and 507.1 ohms, respectively. Consequently, the relay impedance setting increases from 109 to 149 and 379.4 ohms, respectively.

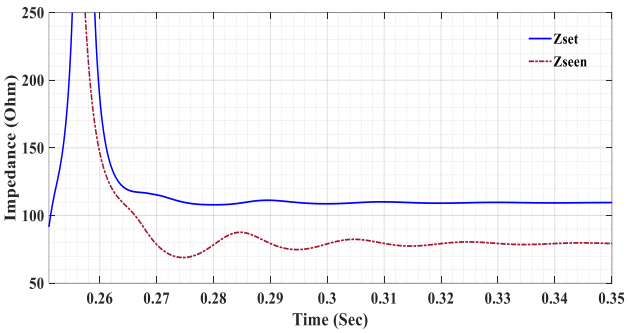



**Fig. 6(a)** occurrence of fault with no resistance

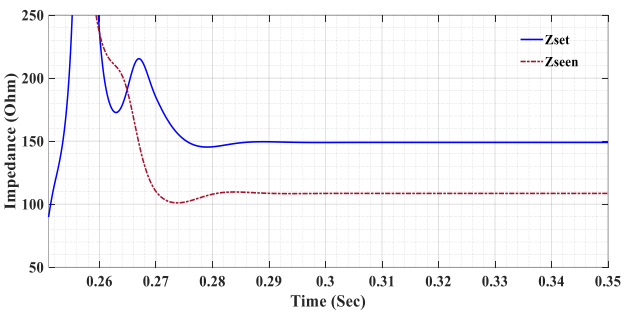



**Fig. 6(b)** fault with a resistance of 50 ohm

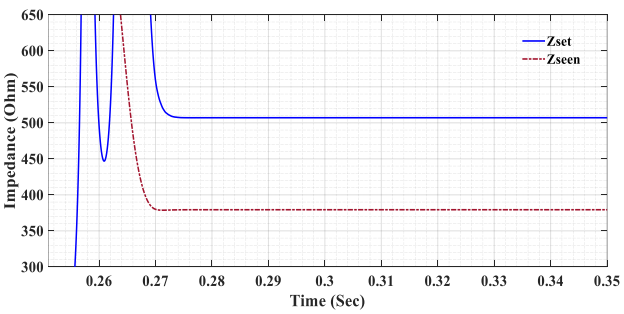



**Fig. 6(c)** .fault with a resistance of 300 ohm

**Fig. 6.** Fault occurrence at 0.75 of transmission line length with different resistances in radial network.

Here, the maximum coverage of the relay is determined for a fault with the highest possible resistance. For this purpose, the fault location is fixed at the end of the transmission line, and the fault resistance is gradually increased so that the relay

impedance setting remains lower than the fault impedance seen by the relay. As shown in Fig. 7, it can be seen that a fault at the end of the transmission line (0.999 of line length) with a resistance of 520 ohms is correctly detected, and the fault impedance seen by the relay is approximately equal to the impedance setting of the relay.

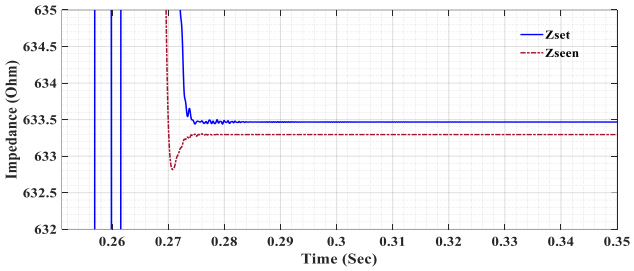



**Fig. 7**: Maximum relay coverage for high-resistance fault occurrence (520 Ohms) in radial network.

### *B. Double-Source Network Configuration*

The overall schematic of the double-source system under study is presented in Fig. 21, and the system specifications are presented in the appendix. To evaluate the performance of the proposed method in this network, some faults with resistances of 0, 50 and 300 ohms in the middle of the transmission line are investigated, and the results are presented in Fig. 8.

In the event of faults with resistances of 0, 50 and 300 ohms in the middle of the transmission line, the fault resistances seen by the relay are 95.6, 164.3 and 700.4 Ohms, respectively. As a result, the adaptive impedances of distance relay setting increase to 195.5, 334.3 and 1392 ohms, respectively. In all cases, the ratio of the fault impedance seen by the relay to the adaptive impedance is maintained around 0.5. Therefore, the process of detecting a fault and locating it for all cases of resistive faults has been correctly completed.

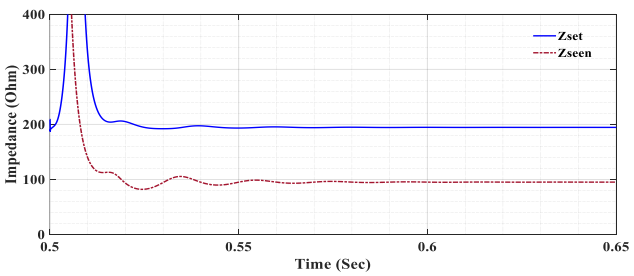



**Fig. 8(a)** occurrence of fault with no resistance

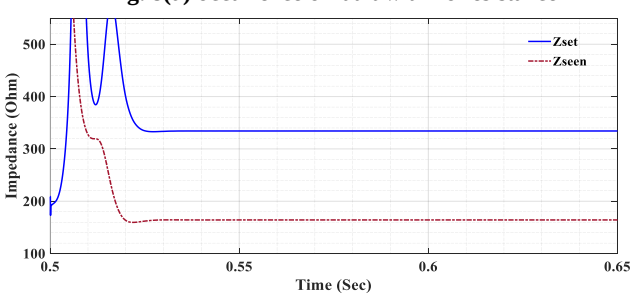



**Fig. 8(b)** fault with a resistance of 50 ohms

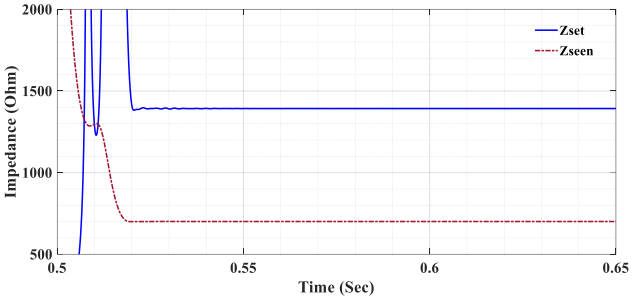



**Fig. 8(c)** fault with a resistance of 300 ohms

**Fig. 8**. Fault occurrence with different resistances at the middle of transmission line in double-source network.

If the fault resistance is 300 ohms, according to Fig. 9, the maximum relay reach is 0.85 of the length of the relay line.

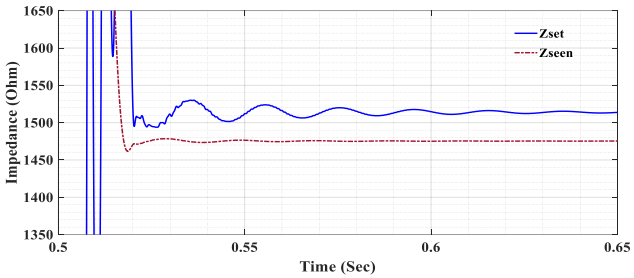



**Fig. 9**. Comparison of impedance setting and the impedance seen by relay for a fault with a resistance of 300 ohms at 0.85 of the transmission line length in double-source configuration.

For the purpose of keeping the relay reach along the entire line, the fault location is fixed at the end of transmission line. Then, the fault resistance is gradually increased so that the relay impedance setting remains lower than the fault impedance seen by the relay. Fig. 10 shows a comparison of these impedances for a fault with a resistance of 8.5 ohms at the end of the transmission line.

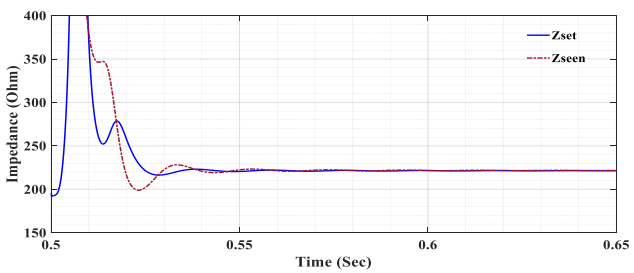



**Fig. 10.** Comparison of impedance setting and the impedance seen by relay for a fault with a resistance of 8.5 ohms at the end of transmission line in double-source configuration.

### *C. Power System Connected to Wind Farms*

The single-line diagram of the power system under study is given in Fig. 11. The system consists of wind farms, transmission lines and the power grid that are connected to each other via transformers. The system consists of three wind farms, each with ten DFIG turbines. A voltage level of 690 V of each turbine increases to 35 kV via a step-up transformer.

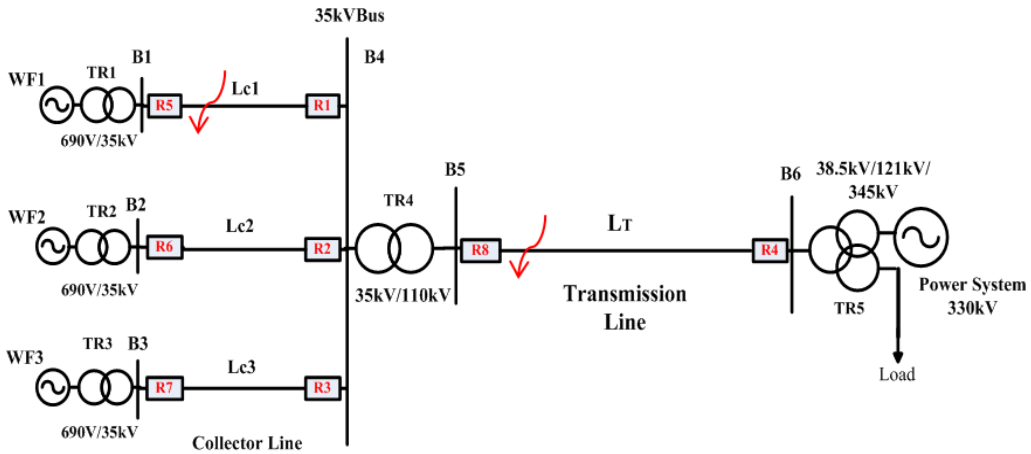



**Fig. 11.** Network under study including wind farms with DFIGs.

The collector line $L_C$ transfer the generated power of each wind farm to a 110 kV step-up transformer to be injected into the power grid via the transmission line $L_T$. The power grid with a voltage level of 330 kV is connected to the transmission line via a three-coil transformer. The voltage level of 35 kV of this transformer is intended to supply local loads. Full specifications of the equipment installed on the system, including lines, wind turbines, power grid and the transformers are given in Tables I-IV.

In this system, the distance relay R4 (on the transmission line side) is the backup of distance relays R1, R2 and R3 (in the collector lines $L_{C1}$, $L_{C2}$ and $L_{C3}$, respectively). Moreover, the distance relay R4 is installed in transmission line $L_T$.

**TABLE I**

SPECIFICATIONS OF LINES OF THE NETWORK UNDER STUDY

| Line label | Rated voltage (kV) | Line length (km) | Positive and negative sequence (Ω) | | Zero sequence (Ω) | |
|---|---|---|---|---|---|---|
| | | | R | X | R | X |
| $L_T$ | 110 | 60 | 0.131 | 0.401 | 0.328 | 0.197 |
| $L_{C1}$ | 35 | 20 | 0.02 | 0.894 | 0.114 | 2.288 |
| $L_{C2}$ | | 14 | | | | |
| $L_{C3}$ | | 8 | | | | |

**TABLE II**

SPECIFICATIONS OF WIND TURBINES

| | Rated Frequency (Hz) | Rated power (MW) | Rated voltage (kV) | Resistance (per unit) | Leakage inductance (per unit) |
|---|---|---|---|---|---|
| Stator | 50 | 2 | 0.69 | 0.0054 | 0.102 |
| Rotor | | | 0.00607 | 0.11 | 4.362 |

**TABLE III**

SPECIFICATIONS OF POWER GRID

| Rated voltage (kV) | Short circuit capacity (MVA) | Positive and negative sequence (Ω) | | Zero sequence (Ω) | |
|---|---|---|---|---|---|
| | | R | X | R | X |
| 330 | 1000 | 4.264 | 85.15 | 0.6 | 9.91 |

**TABLE IV**

SPECIFICATIONS OF TRANSFORMERS OF THE NETWORK UNDER STUDY

| Label | Rated voltage (kV) | | | Rated power (MVA) | R (Ω) | X (Ω) |
|---|---|---|---|---|---|---|
| | Primary | Secondary | Tertiary | | | |
| TR1 | 0.69 | 35 | --- | 25 | 0.91 | 27.23 |
| TR2 | | | | | | |
| TR3 | | | | | | |
| TR4 | 35 | 110 | | 100 | 2.91 | 87.12 |
| TR5 | 110 | 330 | 35 | 150 | 1.09 | 108.9 |

Similarly, relay R8 located on the other side of the transmission line is the backup of relays R5, R6 and R7. Relay R4 has three protection zones. Zone 1 protects the first 80% of the transmission line, zone 2 protects the entire length of the transmission line and the first 50% of the collector lines and zone 3 protects the entire transmission line length and the collector lines. Relay R8 protects only the transmission line, while relays R5, R6 and R7 have three protection zones. Thus, in protection zone 1 of these relays, 80% of the collector lines lengths is protected. In protection zone 2, the entire length of the collector lines and the half-length of the transmission line are protected. Finally, in protection zone 3 of these relays, the entire lengths of the collector and transmission lines are protected.

*D. Setting Protection Zone 1 of Relays*

Relay R8 has one protection zone for the entire transmission line because no coordination with a downstream relay is required. Accordingly, a zero-resistance fault is modeled at the end of the transmission line (close to bus $B_6$), and the impedance seen by relay R8 is then calculated. According to Fig. 12, the impedance setting of this relay is assumed to be 38.86 ohms.

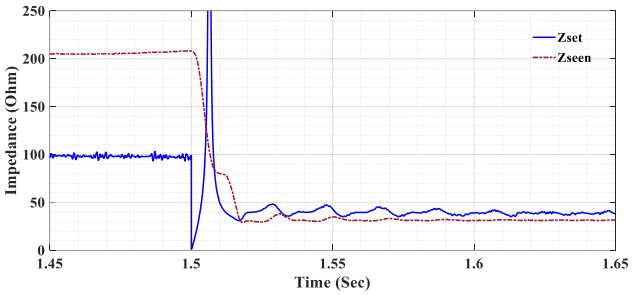



**Fig. 12.** Impedance setting of relay R8 for a fault without resistance at the end of transmission line (close to bus $B_6$).

In the following, due to the similarity of relays R5, R6 and R7, relay R5 is only investigated. Zone 1 of relay R5 protects 80% of the length of line $L_{C1}$. To determine this setting, a zero-resistance fault is exerted at 0.2 of the length of line $L_{C1}$ (close to bus $B_4$). According to Fig. 13, the impedance setting of zone 1 of relay R5 is 21 ohms.

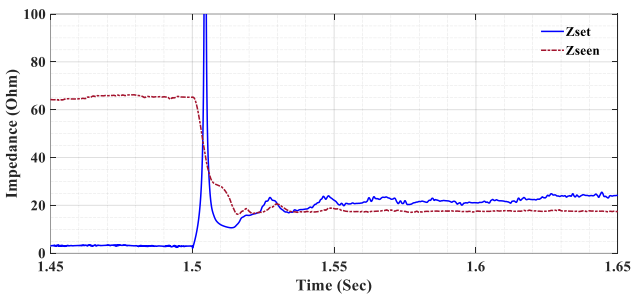



**Fig. 13.** Impedance setting of relay R5 for a fault without resistance at 0.2 of line $L_{C1}$ (close to bus $B_4$).

*E. Setting Protection Zone 2 of Relays*

If the settings of zone 1 of the relays are specified, it is possible to determine the settings of zone 2 of the relays. In this subsection, the settings for other zones of the relays are specified. It is noteworthy that only relays R4, R5, R6 and R7 have zones 2 and 3. Zone 2 of relay R5 covers the entire length of line $L_{C1}$ and half of the transmission line. According to Fig. 14, the impedance setting of zone 2 of R5 is 36 ohms. It is also observed that the fault impedance seen by the relay (35 ohms) is outside the zone 1 and near the boundary of zone 2.

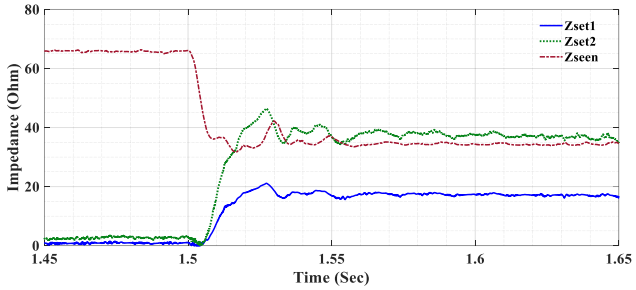



**Fig. 14.** Performance of protection zones 1 and 2 of relay R5 for occurrence of fault without resistance at the middle of transmission line.

In the event of faults at the end of line $L_{C1}$ with resistances 0, 10 and 30 ohms, the fault impedances seen by relay R5 and adaptive settings of zones 1 and 2 of this relay are given in Table V.

**TABLE V**

COMPARISON OF IMPEDANCES OF FAULTS SEEN BY RELAY R5 AND THE IMPEDANCES OF PROTECTION ZONES 1 AND 2.

| Location of fault | End of collector line 1 | | |
|---|---|---|---|
| Value of fault resistance (Ω) | 0 | 10 | 30 |
| Impedance seen by relay | 15.9 | 40.2 | 56.3 |
| Value of adaptive setting of protection zone 1 | 14.8 | 38.2 | 52.3 |
| Value of adaptive setting of protection zone 2 | 32.6 | 84.1 | 116.1 |
| Estimated location of fault occurrence (percentage of line length) | 0.49 | 0.48 | 0.48 |

Based on these results, it can be concluded that, in all cases of resistive faults outside zone 1 (end of line $L_{C1}$), the coordination between zones 1 and 2 of relay R5 is fully maintained because all of the impedances seen by the relay are larger than the adaptive setting of zone 1 and smaller than the setting of zone 2. However, it is observed that, in all cases, the location of fault is determined to be about 48% of the line length, which has a large deviation from the actual location (end of the line). This deviation is due to the branches in this protection zone; that is, the injection of lines $L_{C2}$ and $L_{C3}$ to bus $B_4$ leads to an error in locating the fault.

Next, the fault impedance variations seen by relay R5 and the adaptive impedance of the relay, for a fault at the end of collector line 1 (line $L_{C1}$ close to bus $B_4$) with resistances of 0, 10 and 30 ohms, are illustrated in Fig. 15. As can be seen in Fig. 15, in all cases, the fault impedance seen by the relay is located outside protection zone 1 and inside protection zone 2. In the event of a fault at the end of line $L_{C1}$with resistances 0, 10 and 30 ohms, the amplitudes of the fault impedances seen by the relay and the amplitudes of the adaptive impedance setting of protection zones 1 and 2 of the relay are given in Table V.

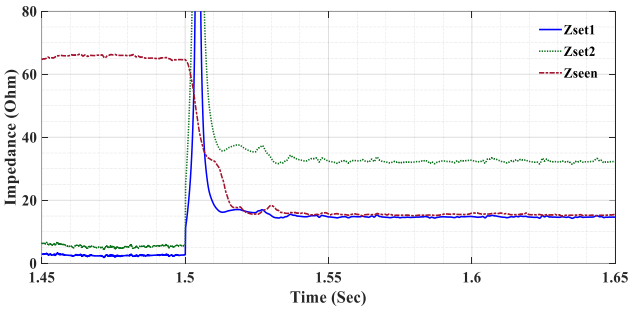



**Fig. 15**(a) occurrence of fault with no resistance

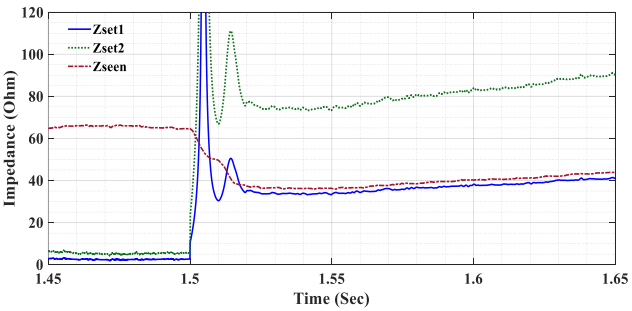



**Fig. 15**(b) fault with a resistance of 10 ohms

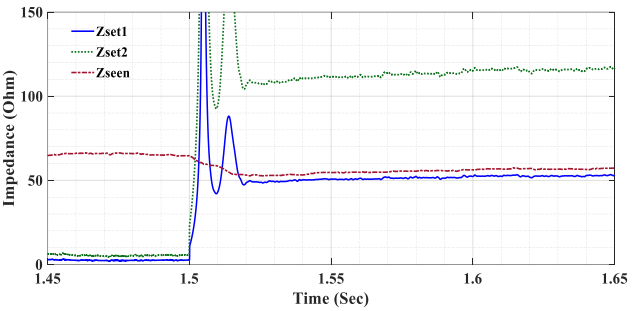



**Fig. 15**(c) fault with a resistance of 30 ohms

**Fig. 15.** Comparison of impedances seen by relay R5 and setting of zones 1 and 2 for a fault at the end of line $L_{C1}$.

The setting of protection zone 2 of relay R4 is determined so that, first, the entire transmission line is covered. Second, the faults that occur within the first 50% of the collector lines can be detected, while these faults are not detectable within the protection zone 1 of relays in the collector lines. Accordingly, the impedance setting of protection zone 2 of relay R4 for a zero resistance fault at the middle of the line $L_{C1}$ is shown in Fig. 16. The amplitudes of the impedance setting and the impedance seen by the relay are approximately 165 ohms.

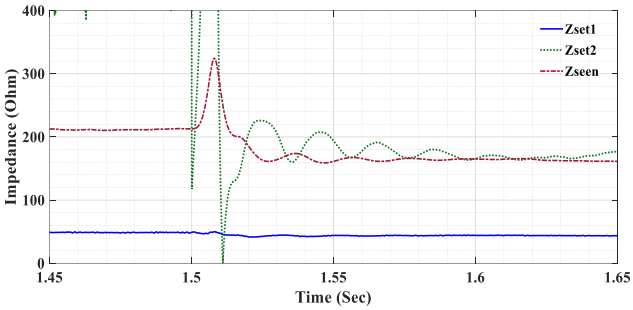



**Fig. 16**: Performance of protection zones 1 and 2 of relay R4 for a zero resistance fault at the middle of line $L_{C1}$

In Fig. 17, the performance of the adaptive method is studied for a resistive fault within protection zone 1 of relay R4. In this figure, two resistive faults of 0 and 10 ohms are generated at the location 20% of line $L_{C1}$at the beginning of this line.

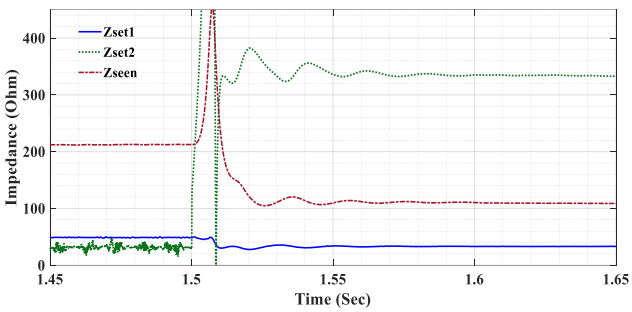



**Fig. 17.(a)** occurrence of fault with no resistance

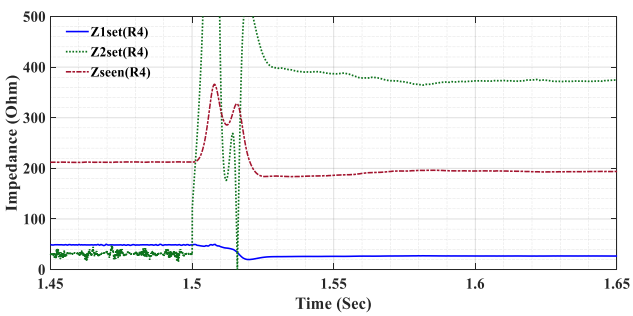



**Fig. 17(b)** fault with a resistance of 10 ohms

**Fig. 17**. Comparison of impedances seen by relay R4 and settings of zones 1 and 2 for a fault at the location 20% of line $L_{C1}$at the beginning of this line.

According to Fig. 17, it is observed that in both cases of fault with and without resistance outside the protection zone 1 of relay R4, the coordination of protection zones 1 and 2 of the relay is maintained. However, the estimation of fault location deviates. This deviation is due to the presence of branches in the path between the locations of relay and fault (i.e., the injection of current by lines $L_{C2}$and $L_{C3}$to bus $B_4$).

*F. Setting Protection Zone 3 of Relays*

If the settings of zone 2 of the relays are specified, it is possible to set zone 3 of the relays. Zone 3 of relay R5 protects the entire lengths of line $L_{C1}$ and the transmission line. Consequently, the impedance setting of this zone is determined as the impedance seen by the relay for zero-resistance fault occurred at the end of the transmission line. The results of this setting are shown in Fig. 18.

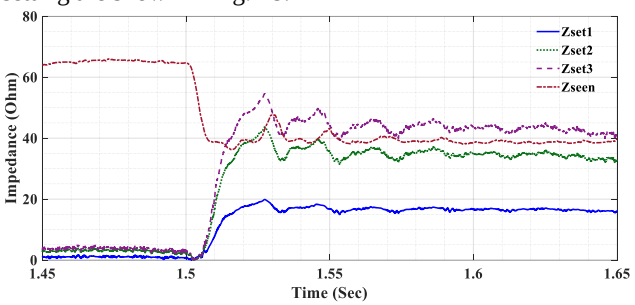



**Fig. 18.** Protection zones 1, 2 and 3 of relay R5 for fault occurrence without resistance at the end of transmission line.

If the relay has multiple protection zones, a predetermined coordination time interval (CTI) must be set between the operating times of these zones to maintain coordination. For example, Fig. 19 illustrates the schematic of the coordination of protection zones 1, 2 and 3 of relay R5 and the operating times of these zones.

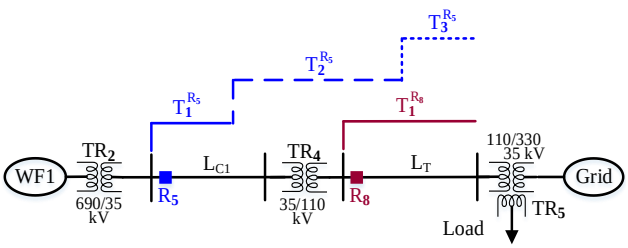



**Fig. 19.** Operation sequence and coordination between relays R5 and R8.

As shown in Fig. 19, in the event of a fault in the first 50% of the transmission line length, relay R8 should act as the primary relay after T1; if, for any reason, relay R8 fails to operate properly, relay R1 should operate as the backup protection at T2 based on its zone 2 settings. Moreover, if a fault occurs in the second half of the transmission line and relay R8 fails to operate at the allowable time T1, relay R5 should operate according to its zone 3 setting at the appropriate time T3. Times T1, T2 and T3 can be equal to 0.01, 0.2 and 0.4 seconds, respectively.

## IV. Conclusions

The performance of conventional distance relays depends on many factors. The most important factor is the fault resistance. In the event of a resistive fault, the line impedance increases and causes distance relays under-reach. This increases the sensibility of distance relays under power fluctuations (the presence of wind farms with DFIG generators). In this paper, an adaptive characteristic was proposed to maintain the accuracy and coordination of distance relays on transmission lines and wind farms collector lines. In this adaptive characteristic, an adaptive coefficient was added to the conventional characteristics to sufficiently increase the relay reach in the case of resistive faults. The proposed adaptive coefficient was defined based on the phasor diagram and the equations of the voltage drop across the fault path so that in the case of a resistive fault, this coefficient was not dependent on the value of the fault resistance. From the numerical results, it was observed that not only the relay sensitivity is maintained for a highly resistive fault (300 ohms), but also the fault location is correctly identified. As a result, the coordination of distance relays on the transmission lines and the DFIG-based wind farm collector lines is also maintained.

## Appendix

*A. Radial Network (Single–Source)*

A radial network structure is shown in Fig. 20, where a load is connected to the power grid at a voltage level of 220 kV via the transmission line. The specifications of the transmission line and the power grid are given in Table VI and VII, respectively.

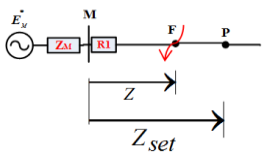



**Fig. 20**. Single-line diagram of radial (Single–source)network.

**TABLE VI**
SPECIFICATIONS OF LINES OF THE NETWORK UNDER STUDY.

| Rated voltage (kV) | Line length (km) | Positive and negative sequence (Ω) | | Zero sequence (Ω) | |
|---|---|---|---|---|---|
| 220 | 150 | R | X | R | X |
| | | 0.029 | 0.362 | 0.255 | 0.971 |

**TABLE VII**
SPECIFICATIONS OF POWER GRID.

| Rated voltage (kV) | Short circuit capacity (MVA) | Positive and negative sequence (Ω) | | Zero sequence (Ω) | |
|---|---|---|---|---|---|
| 220 | 1000 | R | X | R | X |
| | | 4.3578 | 49.8079 | 1.1 | 16.6 |

*B. Double-Source Network*

The structure of a double-source network is shown in Fig. 21, and the specifications are presented in Table VIII and IX. In this network, a 400 km transmission line is connected from both sides to a power grid with a voltage level of 500 kV.

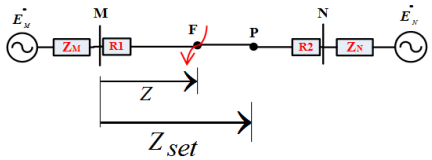



**Fig. 21.** Single-line diagram of double-source network.

**TABLE VIII**

SPECIFICATIONS OF LINES OF THE NETWORK UNDER STUDY.

| Positive and negative sequence | | | Zero sequence | | |
|---|---|---|---|---|---|
| R ($\Omega/km$) | L ($mH/km$) | C ($M\Omega.m$) | R ($\Omega/km$) | L ($mH/km$) | C ($M\Omega.m$) |
| 0.01839 | 0.8376 | 500.1314 | 0.1417 | 1.91943 | 800.5217 |

**TABLE IX**

SPECIFICATIONS OF POWER GRID.

| Short circuit capacity (MVA) | Position | Positive and negative sequence (Ω) | | Zero sequence (Ω) | |
|---|---|---|---|---|---|
| | | R | X | R | X |
| 2500 | Upstream network | 1.05 | 6 | 0.06 | 7.8 |
| | Downstream network | 1.28 | 9 | 6.4 | 18.2 |

## REFERENCES


[1] Z. Li, X. Lin, H. Weng, and Z. Bo, "Efforts on improving the performance of superimposed-based distance protection," *IEEE transactions on power delivery*, vol. 27, no. 1, pp. 186-194, 2012.

[2] V. H. Makwana and B. R. Bhalja, "A new digital distance relaying scheme for compensation of high-resistance faults on transmission line," *IEEE Transactions on Power Delivery*, vol. 27, no. 4, pp. 2133-2140, 2012.

[3] A. Jongepier and L. Van Der Sluis, "Adaptive distance protection of double-circuit lines using artificial neural networks," *IEEE Transactions on Power Delivery*, vol. 12, no. 1, pp. 97-105, 1997.

[4] V. H. Makwana and B. R. Bhalja, "A new adaptive distance relaying scheme for mutually coupled series-compensated parallel transmission lines during intercircuit faults," *IEEE Transactions on power delivery*, vol. 26, no. 4, pp. 2726-2734, 2011.

[5] M. Eissa, "Ground distance relay compensation based on fault resistance calculation," *IEEE Transactions on Power Delivery*, vol. 21, no. 4, pp. 1830-1835, 2006.

[6] J. Ma, W. Ma, Y. Qiu, and J. S. Thorp, "An adaptive distance protection scheme based on the voltage drop equation," *IEEE Transactions on Power Delivery*, vol. 30, no. 4, pp. 1931-1940, 2015.

[7] M. Sanaye-Pasand and P. Jafarian, "An adaptive decision logic to enhance distance protection of transmission lines," *IEEE Transactions on Power Delivery*, vol. 26, no. 4, pp. 2134-2144, 2011.

[8] Liang Y, Lu Z, Li W, Zha W, Huo Y. "A Novel Fault Impedance Calculation Method for Distance Protection Against Fault Resistance," IEEE Transactions on Power Delivery, pp. 1-11, 2019.

[9] H. Zhang and R. Che, "Fault cause identification based on characteristics of transition resistances for transmission lines," in *Electric Utility Deregulation and Restructuring and Power Technologies (DRPT), 2015 5th International Conference on*, 2015, pp. 1405-1409: IEEE.

[10] V. H. Makwana and B. Bhalja, "Distance Relaying Algorithm for a Line-to-ground Fault on Single Infeed Lines," *Electric Power* Components and Systems, vol. 42, no. 12, pp. 1227-1238, 2014.

[11] A. Khajeh and Z. Shabani, "Adaptive Gain Scheduling Control of Doubly Fed Induction Generator Based Wind Turbines to Improve Fault Ride Through Performance," International Journal of Industrial Electronics, Control and Optimization, Vol. 1, No. 1, pp.61-70, June 2018.

[12] Li, B.; Liu, J.; Wang, X.; Zhao, L. "Fault Studies and Distance Protection of Transmission Lines Connected to DFIG-Based Wind Farms," Applied Sciences; 8(4):562, pp. 1-26, 2018.

[13] H. Sadeghi, "A novel method for adaptive distance protection of transmission line connected to wind farms," International Journal of Electrical Power & Energy Systems, vol. 43, no. 1, pp. 1376-1382, 2012.

[14] J. Yang, J. E. Fletcher, and J. O'Reilly, "Multiterminal DC wind farm collection grid internal fault analysis and protection design," IEEE Transactions on Power Delivery, vol. 25, no. 4, pp. 2308-2318, 2010.

[15] S. J. Haslam, P. A. Crossley, and N. Jenkins, "Design and evaluation of a wind farm protection relay," IEE Proceedings-Generation, Transmission and Distribution, vol. 146, no. 1, pp. 37-44, 1999.

[16] A. Han, Z. Zhang, and X. Yin, "The impacts of distributed doubly-fed induction generators on smart distribution Grid protection," in Modelling, Identification and Control (ICMIC), The 2010 International Conference on, pp. 71-75: IEEE, 2010.

[17] B. Wang, X. Dong, and Z. Bo, "Equivalent capacity of the Lower Voltage Ride Through for wind farm from overcurrent protection in power collection lines," 2012.

[18] K. Jia, R. Chen, Z. Xuan, Z. Yang, Y. Fang, and T. Bi, "Fault characteristics and protection adaptability analysis in VSC-HVDC-connected offshore wind farm integration system," IET Renewable Power Generation, vol. 12, no. 13, pp. 1547-1554, 2018.

[19] Chen, Y., Wen, M., Yin, X., Cai, Y., and Zheng, J. "Distance protection for transmission lines of DFIG-based wind power integration system." International Journal of Electrical Power & Energy Systems, vol. 100, pp. 438-448, 2018.

[20] S. Chen, N. Tai, C. Fan, J. Liu, and S. Hong, "Adaptive distance protection for grounded fault of lines connected with doubly-fed induction generators," IET Generation, Transmission & Distribution, vol. 11, no. 6 ,pp. 1513-1520, 2017.

[21] J. Ma, W. Zhang, J. Liu, and J. S. Thorp, "A novel adaptive distance protection scheme for DFIG wind farm collector lines," International Journal of Electrical Power & Energy Systems, vol. 94, pp. 234-244, 2018.



**Jamshid Barati** was born in Baghmalek, Iran, in 1983. He received the B.S. degree from shahid chamran university , Ahvaz, Iran in 2006 and M.Sc. degree from chamran university, ahvaz, Iran in power engineering in 2009. He is currently pursuing towards Ph.D. degree. His areas of research include power system dynamic stability and control, protection relay and FACTS devices.



**Seyed Ghodratollah Seifossadat** was born in Ahwaz, Iran, on August 28,1963 and received the B.Sc. degree in electrical engineering from the Iran University of Science and Technology (IUST), Tehran, in 1989 and the M.Sc. degree in electrical engineering from the Ferdosi University of Mashhad, Mashhad, Iran, in 1992 and the Ph.D. degree from IUST in 2006. Currently, he is with the Department of Engineering, Shahid Chamran University, Ahwaz, Iran, where he has been since 1992. His research interests are power electronics, protection relay, and electric machinery.



**Mahmood Joorabian** was born in Shooshtar, Iran, in 1961. He received Ph.D. degree in electrical engineering from Bath University, England in 1996. He is now a Professor in Electrical Engineering Department of the Engineering Faculty of Shahid Chamran University of Ahvaz, Ahvaz, Iran. His research interests are operation and planning of deregulated power system, load and energy management, renewable energy and smart grids.